Integrated Seat and Suspension Control for a Quarter Car With Driver Model

Haiping Du, Weihua Li, and Nong Zhang

***Abstract*—In this paper, an integrated vehicle seat and suspension control strategy for a quarter car with driver model is proposed to improve suspension performance on driver ride comfort. An integrated seat and suspension model that includes a quarter-car suspension, a seat suspension, and a 4-degree-of-freedom (DOF) driver body model is presented first. This integrated model provides a platform to evaluate ride comfort performance in terms of driver head acceleration responses under typical road disturbances and to develop an integrated control of seat and car suspensions. Based on the integrated model, an H_∞ state feedback controller is designed to minimize the driver head acceleration under road disturbances. Considering that state variables for a driver body model are not measurement available in practice, a static output feedback controller, which only uses measurable state variables, is designed. Further discussion on robust multiobjective controller design, which considers driver body parameter uncertainties, suspension stroke limitation, and road-holding properties, is also provided. Last, numerical simulations are conducted to evaluate the effectiveness of the proposed control strategy. The results show that the integrated seat and suspension control can effectively improve suspension ride comfort performance compared with the passive seat suspension, active seat suspension control, and active car suspension control.**

***Index Terms*—Driver body model, integrated control, seat suspension, static output feedback control, vehicle suspension.**

I. Introduction

SEAT suspension has been commonly accepted in commercial vehicles for industrial, agricultural, and other transport purposes [1] to provide driver ride comfort, reduce driver fatigue due to long hours of driving or exposure to severe working environments such as rough-road conditions, and improve driver safety and health [2]. The study on the optimization and control of seat suspensions for reducing vertical vibration has been an active topic for decades. Three main types of seat suspensions, i.e., passive seat suspension, semiactive seat suspension, and active seat suspension, have been presented so far. The study on passive seat suspension mainly focuses on parameter optimization for the spring stiffness and the damping coefficient. In general, small spring stiffness may get good ride comfort; however, it will incur large suspension deflection and, hence, may cause end-stop collision. Studies on minimum stiffness in terms of seat position [3] and nonlinear stiffness [4] have been conducted to compromise ride comfort and suspension deflection limitation. With the development of magnetorheological (MR) or electrorheological (ER) dampers, semiactive control of seat suspension has been proposed to provide variable damping force with less power consumption [1], [5]. However, either ER or MR fluid only has controllable-damping capability such that the system is effective only during the energy dissipation stage. The study on active seat suspension mainly focuses on developing advanced control strategies or applying different types of actuators to improve seat suspension performance while taking into account issues such as actuator saturation, load variation, time delay, and reliability [6]–[11]. Among the three types of seat suspension, active seat suspension can provide the best ride comfort performance and has therefore received much more attention in recent years.

In addition to seat suspension, vehicle suspension has extensively been studied for a long time [12]. Vehicle suspension is, in fact, designed as a primary suspension for all vehicles to provide ride comfort, road holding, and other dynamic functions. Similar to seat suspension, passive, semiactive, and active vehicle suspensions have also been proposed. Active and semiactive suspensions attracted more attention in both the academe and the industry for improving vehicle ride comfort and road holding [13]–[15]. In particular, the active electromagnetic suspension system presents an impressive perspective for the implementation of active suspension to passenger vehicles [16]–[20]. However, it is noticed that most of the current active and semiactive seat suspension and active and semiactive vehicle suspension are separately designed or studied, although their common function is to improve the vehicle ride comfort performance. It is therefore natural to think about the question: Should suspension be integrally controlled to provide an enhanced ride comfort performance? This question motivates this paper.

To achieve an enhanced ride comfort performance, an integrated seat and suspension model that includes a quarter-car suspension [2-degree-of-freedom (DOF)], a seat suspension (2 DOF), and a driver body model (4 DOF) is first developed in this paper. Developing such an integrated model is twofold: It will be used to design an integrated controller that provides control forces to both car suspension and seat suspension, and typical road disturbances can be applied to the vehicle tire instead of the cabin to evaluate the suspension performance. This is more reasonable, because road signals must be filtered by vehicle

Manuscript received June 9, 2011; revised September 16, 2011, February 26, 2012, and May 18, 2012; accepted July 25, 2012. Date of publication August 8, 2012; date of current version November 6, 2012. This work was supported in part by the University of Wollongong through the URC Small Grant Scheme. The review of this paper was coordinated by Dr. S. Anwar.

H. Du is with the School of Electrical, Computer and Telecommunications Engineering, University of Wollongong, Wollongong, NSW 2522, Australia (e-mail: hdu@uow.edu.au).

W. Li is with the School of Mechanical, Materials and Mechatronic Engineering, University of Wollongong, Wollongong, NSW 2522, Australia.

N. Zhang is with the Faculty of Engineering and Information Technology, University of Technology, Sydney, NSW 2007, Australia.

Color versions of one or more of the figures in this paper are available online at http://ieeexplore.ieee.org.

Digital Object Identifier 10.1109/TVT.2012.2212472

suspension in both amplitude and frequency components when getting to the cabin. Directly applying typical road disturbances to the cabin to evaluate the seat suspension performance may not be appropriate, particularly when studying issues such as actuator saturation and suspension deflection limitation, which are generally subject to the applied inputs. In addition, the suspension performance on ride comfort can be evaluated in terms of a human body model instead of sprung mass, because sprung mass acceleration cannot fully reflect the human body biomechanical effect on ride comfort. Currently, only a few studies [21], [22] consider both vehicle suspension and seat suspension together to study the vehicle or seat suspension optimization problem. Based on the integrated model, an H_∞ state feedback controller is then designed for the integrated seat and suspension model to generate the desired control forces for reducing driver head acceleration under energy-bounded road inputs and actuator saturation constraints. Then, a static output feedback controller is designed, considering that not all state variables, particularly the state variables in relation to the human body model, are not measurement available in practice. Then, a robust controller design that considers parameter uncertainties and performance requirements on suspension stroke and road-holding properties is further discussed. Last, numerical simulations are used to validate the effectiveness of the proposed control strategy by comparing it with passive seat suspension, active seat suspension control, and active car suspension control.

This paper is organized as follows. In Section II, the integrated seat and suspension model is developed. In Section III, controller design approaches for the proposed model will be presented, where a controller design procedure for a nominal system with one objective on ride comfort is first discussed, and then, a robust controller design for an uncertain system with three objectives is further discussed. The simulation results will be shown in Section IV. Finally, conclusions are summarized in Section V.

The notation used throughout this paper is standard. For a real symmetric matrix W, $W > 0$ ($W < 0$) is used to denote its positive-definiteness (negative-definiteness). $\|\cdot\|$ refers to either the Euclidean vector norm or the induced matrix 2-norm. I is used to denote the identity matrix of appropriate dimensions. To simplify the notation, $*$ is used to represent a block matrix that is readily inferred by symmetry.

II. Integrated Vehicle Seat and Suspension Model

The integrated vehicle seat and suspension model includes a quarter-car suspension model, a seat suspension model, and a 4-DOF driver body model, as shown in Fig. 1, where m_s is the sprung mass, which represents the car chassis; m_u is the unsprung mass, which represents the wheel assembly; m_f is the seat frame mass; m_c is the seat cushion mass; and the driver body is composed of four mass segments, i.e., thighs m_1, lower torso m_2, high torso m_3, and head m_4, where the arms and legs are combined with the upper torso and thighs, respectively. z_u, z_s, z_f, z_c, and $z_{1\sim4}$ are the displacements of the corresponding masses, respectively, and z_r is the road displacement input. c_s and k_s are the damping and stiffness of the car suspension system, respectively, k_t and c_t stand for the compressibility and damping of the pneumatic tire, respectively. c_s, c_{ss}, $c_{1\sim4}$, k_s, k_{ss}, and $k_{1\sim4}$ are defined in Table I. u_s and u_f represent the active control forces that are applied to the car suspension and the seat suspension, respectively. In practice, electrohydraulic actuators or linear permanent-magnet motors could be applied to generate the required forces u_s and u_f.

The dynamic vertical motion of equations for the quarter-car suspension, seat suspension, and driver body are given by

$$\begin{aligned} m_u\ddot{z}_u =& -k_t(z_u - z_r) - c_t(\dot{z}_u - \dot{z}_r) \\ &+ k_s(z_s - z_u) + c_s(\dot{z}_s - \dot{z}_u) + u_s \quad (1)\\ m_s\ddot{z}_s =& -k_s(z_s - z_u) - c_s(\dot{z}_s - \dot{z}_u) \\ &+ k_{ss}(z_f - z_s) + c_{ss}(\dot{z}_f - \dot{z}_s) - u_s + u_f \quad (2)\\ m_f\ddot{z}_f =& -k_{ss}(z_f - z_s) - c_{ss}(\dot{z}_f - \dot{z}_s) \\ &+ k_c(z_c - z_f) + c_c(\dot{z}_c - \dot{z}_f) - u_f \quad (3)\\ m_c\ddot{z}_c =& -k_c(z_c - z_f) - c_c(\dot{z}_c - \dot{z}_f) \\ &+ k_1(z_1 - z_c) + c_1(\dot{z}_1 - \dot{z}_c) \quad (4)\\ m_1\ddot{z}_1 =& -k_1(z_1 - z_c) - c_1(\dot{z}_1 - \dot{z}_c) \\ &+ k_2(z_2 - z_1) + c_2(\dot{z}_2 - \dot{z}_1) \quad (5)\\ m_2\ddot{z}_2 =& -k_2(z_2 - z_1) - c_2(\dot{z}_2 - \dot{z}_1) \\ &+ k_3(z_3 - z_2) + c_3(\dot{z}_3 - \dot{z}_2) \quad (6)\\ m_3\ddot{z}_3 =& -k_3(z_3 - z_2) - c_3(\dot{z}_3 - \dot{z}_2) \\ &+ k_4(z_4 - z_3) + c_4(\dot{z}_4 - \dot{z}_3) \quad (7)\\ m_4\ddot{z}_4 =& -k_4(z_4 - z_3) - c_4(\dot{z}_4 - \dot{z}_3). \quad (8) \end{aligned}$$

Note that the quarter-car suspension model (1) and (2), with $k_{ss} = 0$, $c_{ss} = 0$, and $u_f = 0$, has been used by many researchers in studying the active or semiactive control of vehicle suspensions. The seat suspension model (3) and (4) or the seat suspension with driver body model (3)–(8), with $k_s = 0$, $c_s = 0$, and $z_s = z_r$, has been applied in studying active or semiactive seat suspension control. An integrated model (1)–(3) or (1)–(4), with $u_s = 0$ and $u_f = 0$, has been used in studying the seat or suspension optimization problem [21], [22]. Currently, no integrated model (1)–(8) has been found in the literature to study active seat and suspension control together.

By defining the following set of state variables, $x_1 = z_u - z_r$, $x_2 = \dot{z}_u$, $x_3 = z_s - z_u$, $x_4 = \dot{z}_s$, $x_5 = z_f - z_s$, $x_6 = \dot{z}_f$, $x_7 = z_c - z_f$, $x_8 = \dot{z}_c$, $x_9 = z_1 - z_c$, $x_{10} = \dot{z}_1$, $x_{11} = z_2 - z_1$, $x_{12} = \dot{z}_2$, $x_{13} = z_3 - z_2$, $x_{14} = \dot{z}_3$, $x_{15} = z_4 - z_3$, and $x_{16} = \dot{z}_4$, the state vector $x = [x_1 \quad x_2 \quad \cdots \quad x_{16}]^T$, the control input vector, $u = [u_f \quad u_s]^T$, and the road disturbance $w = \dot{z}_r$, we can write the dynamic equations (1)–(8) into state-space form as

$$\dot{x} = Ax + B_w w + Bu \quad (9)$$

where matrices A, B_w, and B can be obtained from (1)–(8).

In practice, all the actuators are limited by their physical capabilities, and hence, actuator saturation needs to be considered for the active control of seat suspension [10] and car suspension [23].Taking actuator saturation into account, (9) is modified as

$$\dot{x} = Ax + B_w w + B\bar{u} \quad (10)$$

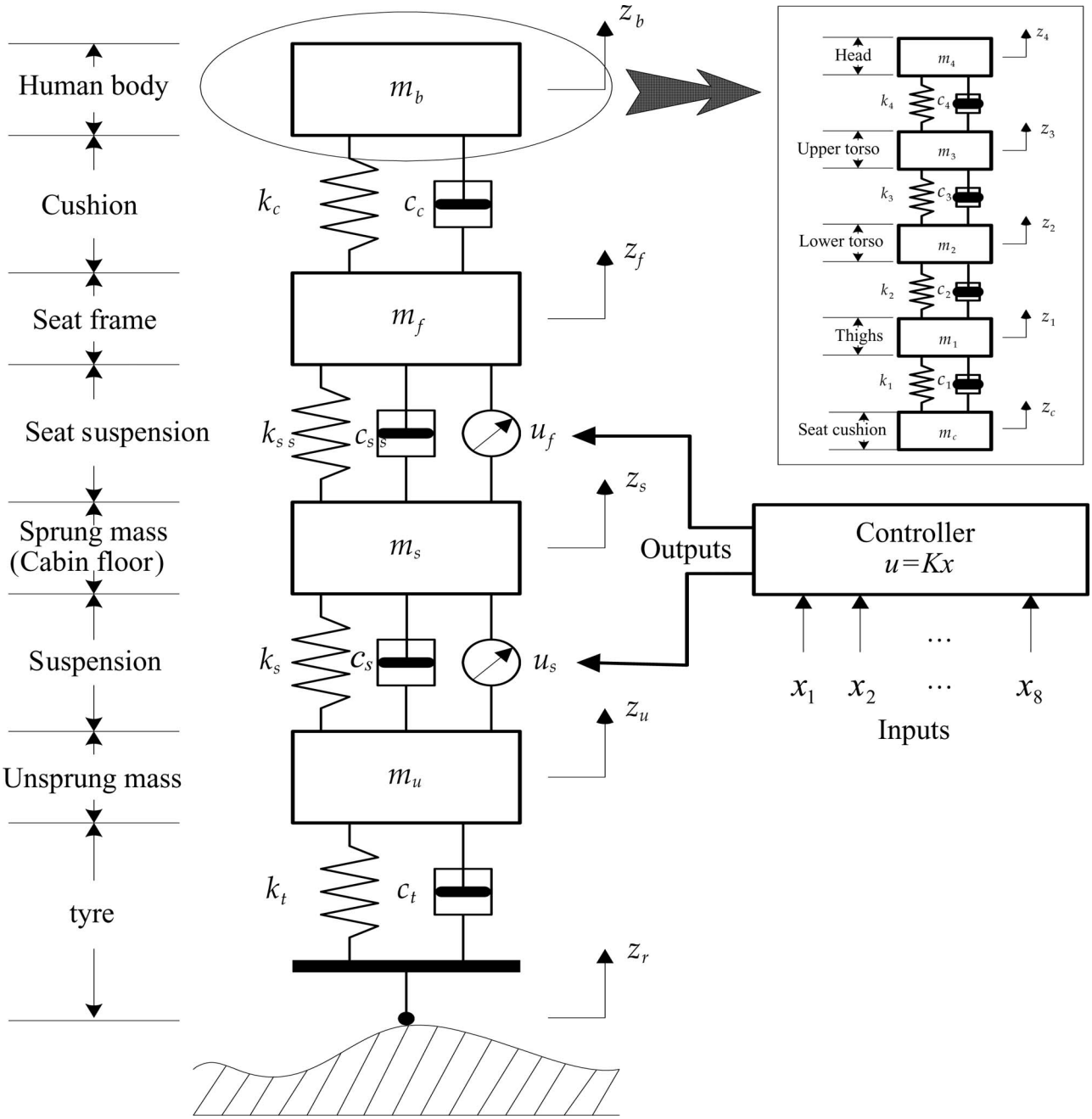

Fig. 1. Integrated seat and suspension model.

TABLE I
PARAMETERS OF THE SEAT–DRIVER SUSPENSION MODEL

c_{ss}	damping of seat suspension	k_{ss}	stiffness of seat suspension
c_c	damping of seat cushion	k_c	stiffness of seat cushion
c_1	damping of buttocks and thighs	k_1	stiffness of buttocks and thighs
c_2	damping of lumber spine	k_2	stiffness of lumber spine
c_3	damping of thoracic spine	k_3	stiffness of thoracic spine
c_4	damping of cervical spine	k_4	stiffness of cervical spine

where $\bar{u} = \text{sat}(u)$, and $\text{sat}(u)$ is a saturation function of control input u, defined as

$$\text{sat}(u) = \begin{cases} -u_{\lim}, & \text{if } u < -u_{\lim}, \\ u, & \text{if } -u_{\lim} \leqslant u \leqslant u_{\lim} \\ u_{\lim}, & \text{if } u > u_{\lim} \end{cases} \tag{11}$$

where $u_{\lim}$ is the control input limit.

To deal with the saturation problem in the controller design process, the following lemma will be used.

Lemma 1 [24]: For the saturation constraint that was defined by (11), as long as $|u| \leqslant (u_{\lim}/\varepsilon)$, we have

$$\left\| \bar{u} - \frac{1+\varepsilon}{2} u \right\| \leqslant \frac{1-\varepsilon}{2} \|u\| \tag{12}$$

and hence

$$\left[\bar{u} - \frac{1+\varepsilon}{2} u \right]^T \left[\bar{u} - \frac{1+\varepsilon}{2} u \right] \leqslant \left(\frac{1-\varepsilon}{2} \right)^2 u^T u \tag{13}$$

where $0 < \varepsilon < 1$ is a given scalar.

To apply Lemma 1 in the next section, (10) is further written as

$$\begin{aligned}\dot{x} &= Ax + B_w w + B\frac{1+\varepsilon}{2}u + B\left(\bar{u} - \frac{1+\varepsilon}{2}u\right)\\ &= Ax + B_w w + B\frac{1+\varepsilon}{2}u + Bv \end{aligned} \tag{14}$$

where $v = \bar{u} - (1+\varepsilon/2)u$.

To derive the main result, the following lemma is also used.

Lemma 2 [25]: For any matrices (or vectors) X and Y with appropriate dimensions, we have

$$X^T Y + Y^T X \leqslant \epsilon X^T X + \epsilon^{-1} Y^T Y \tag{15}$$

where $\epsilon > 0$ is any scalar.

III. Controller Design

To improve the system performance, a state feedback controller is designed as

$$u = Kx \tag{16}$$

where K is the feedback gain matrix to be designed. It is shown that the input to the controller is the state vector x and the output of the controller is the control force vector u, which is also the control input to the system (10). Once K is known, u can be calculated using (16). For further understanding, Fig. 1 shows a block diagram of the controller, of which inputs are the state variables x_1 to x_8, which are assumed to be measurable in practice as an example, and outputs are u_s and u_f.

For the car and seat suspension design, the performance on ride comfort is mainly described by the driver head acceleration [9], [11] and, therefore, the driver head acceleration as

$$z = \ddot{z}_4 = Cx \tag{17}$$

where C is the last row of matrix A, which is defined as the control output.

To achieve good ride comfort and make the controller adequately perform for a wide range of road disturbances, the L_2 gain between the road disturbance input w and the control output z is defined as

$$\|T_{zw}\|_\infty = \sup_{w\neq 0} \frac{\|z\|_2}{\|w\|_2} \tag{18}$$

where $\|z\|_2^2 = \int_0^\infty z^T(t)z(t)dt$, and $\|w\|_2^2 = \int_0^\infty w^T(t)w(t)dt$, is chosen as the performance measure. A small value of $\|T_{zw}\|_\infty$ generally means a small value of driver head acceleration under energy-limited road disturbances. Therefore, the control objective is to design a controller (16) such that the closed-loop system, which is composed by substituting (16) into (10), is asymptotically stable and the performance measure (18) is minimized.

A. Controller Design for a Nominal System

To design such a controller, we now define a Lyapunov function for (10), which is assumed to be a nominal system without parameter uncertainties, as

$$V(x) = x^T P x \tag{19}$$

where P is a positive-definite matrix. By differentiating (19) and using (14), we obtain

$$\begin{aligned}\dot{V}(x) &= \dot{x}^T P x + x^T P \dot{x}\\ &= \left[Ax + B_w w + B\frac{1+\varepsilon}{2}u + Bv\right]^T Px + x^T(t)P\\ &\quad\times\left[Ax + B_w w + B\frac{1+\varepsilon}{2}u + Bv\right].\end{aligned} \tag{20}$$

By using Lemma 1, Lemma 2, and (16), we have

$$\begin{aligned}\dot{V}(x) &\leqslant x^T\left[A^TP + PA + \left(B\frac{1+\varepsilon}{2}K\right)^T P + PB\frac{1+\varepsilon}{2}K\right]x\\ &\quad + w^T B_w^T Px + x^T PB_w w + \epsilon v^T v + \epsilon^{-1}x^T PBB^T Px\\ &\leqslant x^T\left[A^TP + PA + \left(B\frac{1+\varepsilon}{2}K\right)^T P + PB\frac{1+\varepsilon}{2}K\right]x\\ &\quad + w^T B_w^T Px + x^T PB_w w\\ &\quad + \epsilon\left(\frac{1-\varepsilon}{2}\right)^2 u^T u + \epsilon^{-1}x^T PBB^T Px\\ &= x^T\Theta x + w^T B_w^T Px + x^T PB_w w.\end{aligned} \tag{21}$$

Here

$$\begin{aligned}\Theta = \Bigg[&A^TP + PA + \left(B\frac{1+\varepsilon}{2}K\right)^T P + PB\frac{1+\varepsilon}{2}K\\ &+\epsilon\left(\frac{1-\varepsilon}{2}\right)^2 K^T K + \epsilon^{-1}PBB^T P\Bigg]\end{aligned}$$

and ϵ is any positive scalar.

Adding $z^T z - \gamma^2 w^T w$, $\gamma > 0$, which is a performance index, to the two sides of (21) yields

$$\begin{aligned}&\dot{V}(x) + z^T z - \gamma^2 w^T w\\ &\quad\leqslant \begin{bmatrix} x^T & w^T\end{bmatrix}\begin{bmatrix}\Theta + C^T C & PB_w\\ B_w^T P & -\gamma^2 I\end{bmatrix}\begin{bmatrix}x\\ w\end{bmatrix}\\ &\quad= \begin{bmatrix} x^T & w^T\end{bmatrix}\Pi\begin{bmatrix}x\\ w\end{bmatrix}\end{aligned} \tag{22}$$

where $\Pi = \begin{bmatrix}\Theta + C^T C & PB_w\\ B_w^T P & -\gamma^2 I\end{bmatrix}$.

Based on (22), it is now deduced that, if $\Pi < 0$, then $\dot{V}(x) + z^T z - \gamma^2 w^T w < 0$, and $\|T_{zw}\|_\infty < \gamma$ with the initial condition $x(0) = 0$ [26]. When the road disturbance is zero, i.e., $w = 0$, based on (22), it can be inferred that, if $\Pi < 0$, then $\dot{V}(x) < 0$, and (10) with the controller (16) is quadratically stable.

By premultiplying and postmultiplying Π with $\mathrm{diag}(P^{-1} \quad I)$ and its transpose, respectively, and defining $Q = P^{-1}$ and $Y = KQ$, the condition of $\Pi < 0$ is equivalent to

$$\begin{bmatrix} QA^T + AQ + \frac{1+\varepsilon}{2}Y^T B^T & \\ +\frac{1+\varepsilon}{2}BY + \epsilon\left(\frac{1-\varepsilon}{2}\right)^2 Y^T Y & B_w\\ +\epsilon^{-1}BB^T + QC^T CQ & \\ B_w^T & -\gamma^2 I\end{bmatrix} < 0. \tag{23}$$

By the Schur complement, (23) is equivalent to (24), shown at the bottom of the page.

On the other hand, based on (16), the constraint $|u| \leqslant (u_{\lim}/\varepsilon)$ can be expressed as

$$|Kx| \leqslant \frac{u_{\lim}}{\varepsilon}. \tag{25}$$

Let $\Omega(K) = \{x||x^T K^T K x| \leqslant (u_{\lim}/\varepsilon)^2\}$. Then, the equivalent condition for an ellipsoid $\Omega(P,\rho) = \{x|x^T P x \leqslant \rho\}$ being a subset of $\Omega(K)$, i.e., $\Omega(P,\rho) \subset \Omega(K)$, is given as [27]

$$K\left(\frac{P}{\rho}\right)^{-1} K^T \leqslant \left(\frac{u_{\lim}}{\varepsilon}\right)^2. \tag{26}$$

By the Schur complement, (26) can be written as

$$\begin{bmatrix} \left(\frac{u_{\lim}}{\varepsilon}\right)^2 I & K\left(\frac{P}{\rho}\right)^{-1} \\ \left(\frac{P}{\rho}\right)^{-1} K^T & \left(\frac{P}{\rho}\right)^{-1} I \end{bmatrix} \geqslant 0. \tag{27}$$

Using the definitions $Q = P^{-1}$ and $Y = KQ$, (27) is equivalent to

$$\begin{bmatrix} \left(\frac{u_{\lim}}{\varepsilon}\right)^2 I & Y \\ Y^T & \rho^{-1} Q \end{bmatrix} \geqslant 0. \tag{28}$$

The controller design problem is now summarized as follows. For given numbers $\gamma > 0$, $\varepsilon > 0$, $\rho > 0$, and $u_{\lim}$, (10) with the controller (16) is quadratically stable, and $\|T_{zw}\|_\infty < \gamma$ if there exist matrices $Q > 0$, Y and a scalar $\epsilon > 0$ such that linear matrix inequalities (LMIs) (24) and (28) are feasible. Moreover, the feedback gain matrix is obtained as $K = YQ^{-1}$.

It is noticed that (24) and (28) are LMIs to γ^2; hence, to minimize the performance measure γ, the controller design problem can be modified as a minimization problem of

$$\min \gamma^2 \text{ s.t. LMIs (24) and (28).} \tag{29}$$

This minimization problem is a convex optimization problem and can be solved by using some available software such as the MATLAB LMI Toolbox. Because the solution to (29) will be dependent on the values of ε and ρ, it is a suboptimal solution for a given $u_{\lim}$. Choosing values for ε and ρ is a trial-and-error process. In general, using small values of ε and ρ may get a high-gain controller design.

Note that the aforementioned state feedback controller assumes that all the state variables are measurement available. This case is not true, particularly when considering a high-DOF human body model where most of the state variables, e.g., torso displacements and velocities, are not measurable or not suitable for measurement when a driver is driving. Therefore, a control strategy that uses only available measurements needs to be developed. An observer-based output feedback or dynamic output feedback [11] could be applied using the available measurements; however, it makes the design and implementation tasks expensive and hard, particularly when the model order (even after model reduction [5]) is higher. On the contrary, controllers that use static output feedback are less expensive to implement and are more reliable. Therefore, a static output feedback controller will further be considered for the integrated seat and suspension control. A static output feedback controller is a challenging issue from both the analytical and numerical points of view due to its nonconvex nature [28]. Although genetic algorithms can be applied to design a static output feedback controller [29], a computationally efficient numerical algorithm [30] will be applied here.

The static output feedback controller is designed as

$$u = KC_s x \tag{30}$$

where C_s is used to define the available state variables. For example, if only x_1 in (9) is available for feedback, then C_s is defined as $C_s = [1 \quad [0]_{1\times 15}]$.

By using (30) instead of (16) in (20), defining $WC_s = C_s Q$ and $Y = KW$, and following a similar procedure as derived for the state feedback controller design, we can get the conditions as given in (31) and (32), shown at the bottom of the page, which are similar to (24) and (28), respectively, for the static output feedback controller design. In addition, the static output feedback gain matrix is obtained as $K = YW^{-1}$.

$$\begin{bmatrix} QA^T + AQ + \frac{1+\varepsilon}{2}[Y^T B^T + BY] + \epsilon^{-1} BB^T & Y^T & QC^T & B_w \\ * & -\epsilon^{-1}\left(\frac{2}{1-\varepsilon}\right)^2 I & 0 & 0 \\ * & * & -I & 0 \\ * & * & * & -\gamma^2 I \end{bmatrix} < 0 \tag{24}$$

$$\begin{bmatrix} QA^T + AQ + \frac{1+\varepsilon}{2}\left[C_s^T Y^T B^T + BYC_s\right] + \epsilon^{-1} BB^T & C_s^T Y^T & QC^T & B_w \\ * & -\epsilon^{-1}\left(\frac{2}{1-\varepsilon}\right)^2 I & 0 & 0 \\ * & * & -I & 0 \\ * & * & * & -\gamma^2 I \end{bmatrix} < 0 \tag{31}$$

$$\begin{bmatrix} \left(\frac{u_{\lim}}{\varepsilon}\right)^2 & YC_s \\ C_s^{\bar{T}} Y^T & \rho^{-1} Q \end{bmatrix} \geqslant 0 \tag{32}$$

It is observed that the static output feedback controller design is the feasibility problem of LMIs (7) and (32) with the equality constraint $WC_s = C_sQ$. The equality constraint $WC_s = C_sQ$ can equivalently be converted to [31]

$$\text{tr}\left[(WC_s - C_sQ)^T(WC_s - C_sQ)\right] = 0. \tag{33}$$

By introducing the condition

$$(WC_s - C_sQ)^T(WC_s - C_sQ) \leqslant \mu I \tag{34}$$

where $\mu > 0$, it is then equivalent to

$$\begin{bmatrix} -\mu I & (WC_s - C_sQ)^T \\ WC_s - C_sQ & -I \end{bmatrix} \leqslant 0 \tag{35}$$

through the Schur complement. If we assume that μ is a very small positive number, e.g., 10^{-10}, then we can numerically design a static output feedback controller by solving the following minimization problem:

$$\min \gamma^2 \text{ s.t. to LMIs (31), (32), and (35).} \tag{36}$$

B. Robust Multiobjective Controller Design

In practice, the mass of the driver body may be varied when a driver's physical condition is changed or a different driver who has a different weight is driving the vehicle. To make the controller have similar performance despite the changes of the driver's mass, the variation to the driver's mass will be considered. Referring to the driver model that was used in this paper, it is shown that the driver's mass is composed of the masses of the thighs, lower torso, high torso, and head, i.e., $m = \sum_{i=1}^{4} m_i$. It is reasonable to assume that the mass variation ratio to each segment of the driver body is equal and the driver's mass is, in fact, varied in a range of $[m_{\min}, m_{\max}]$, where $m_{\min}$ and $m_{\max}$ are the possible minimum and maximum driver's masses, respectively. Therefore, it is not difficult to represent the uncertain driver's mass that appeared in the model as

$$\frac{1}{m} = h_1 \frac{1}{m_{\min}} + h_2 \frac{1}{m_{\max}} \tag{37}$$

where h_1 and h_2 are defined as

$$h_1 = \frac{1/m - 1/m_{\max}}{1/m_{\min} - 1m_{\max}}, \quad h_2 = \frac{1/m_{\max} - 1/m}{1/m_{\min} - 1/m_{\max}}. \tag{38}$$

It is shown that $h_i \geqslant 0$, $i = 1, 2$, and $\sum_{i=1}^{2} h_i = 1$. If we define $m_{\min} = (1-\delta)m = \delta_{\min} m = \delta_{\min} \sum_{i=1}^{4} m_i$, $m_{\max} = (1+\delta)m = \delta_{\max} m = \delta_{\max} \sum_{i=1}^{4} m_i$, where $0 < \delta < 1$, $\delta_{\min} = 1 - \delta$, and $\delta_{\max} = 1 + \delta$, the vehicle model in (10) with an uncertain driver's mass can be expressed as

$$\dot{x} = \sum_{i=1}^{2} h_i A_i x + B_w w + B\bar{u} \tag{39}$$

where matrices A_i, $i = 1, 2$ are obtained by replacing m_j, $j = 1, 2, 3, 4$ in matrix A with $\delta_{\min} m_j$ and $\delta_{\max} m_j$, respectively.

On the other hand, parameter uncertainties may happen to the damping coefficient and stiffness of each segment of the driver body, of which values are, in fact, hard to accurately measure in practice. To describe these uncertainties in the model, a norm-bounded method can be used. Let us assume that the stiffness and damping coefficient with uncertainties can be described as $k = k_o(1 + d_k\delta_k)$ and $c = c_o(1 + d_c\delta_c)$, respectively, where k_o and c_o are the nominal values, δ_k and δ_c are the uncertainties, with $|\delta_k| \leqslant 1$ and $|\delta_c| \leqslant 1$, and d_k (d_c) indicates the percentage of variation that is allowed for a given parameter around its nominal value. Then, taking a matrix T with uncertain k and c as an example, it can be expressed as

$$\begin{aligned} T &= \begin{bmatrix} k & c \\ \# & \# \end{bmatrix} = \begin{bmatrix} k_o(1 + d_k\delta_k) & c_o(1 + d_c\delta_c) \\ \# & \# \end{bmatrix} \\ &= \begin{bmatrix} k_o & c_o \\ \# & \# \end{bmatrix} + \begin{bmatrix} 1 & 1 \\ 0 & 0 \end{bmatrix} \begin{bmatrix} \delta_k & 0 \\ 0 & \delta_c \end{bmatrix} \begin{bmatrix} d_k k_o & 0 \\ 0 & d_c c_o \end{bmatrix} \\ &= T_o + HFE \end{aligned}$$

where $T_o = \begin{bmatrix} k_o & c_o \\ \# & \# \end{bmatrix}$, $H = \begin{bmatrix} 1 & 1 \\ 0 & 0 \end{bmatrix}$, $E = \begin{bmatrix} d_k k_o & 0 \\ 0 & d_c c_o \end{bmatrix}$, $F = \begin{bmatrix} \delta_k & 0 \\ 0 & \delta_c \end{bmatrix}$, with $F^T F \leqslant I$, and # represents an arbitrary element in the matrix. Following a similar principle, (39) with parameter uncertainties on stiffness and damping coefficients can be expressed as

$$\dot{x} = \sum_{i=1}^{2} h_i (A_i + \Delta A_i) x + B_w w + B\bar{u} \tag{40}$$

where $\Delta A_i = H_a F E_i$ represents the uncertainty that was caused by the uncertain stiffness and damping coefficients on matrix A_i, H_a and E_i are known constant matrices with appropriate dimensions, which can be defined in terms of the locations and variation ranges of the uncertain parameters that appeared in matrix A_i, and F is an unknown matrix function that is bounded by $F^T F \leqslant I$. For description simplicity, we define $A_h = \sum_{i=1}^{2} h_i A_i$, $\Delta A_h = \sum_{i=1}^{2} h_i \Delta A_i = \sum_{i=1}^{2} h_i H_a F E_i = H_a F E_h$, where $E_h = \sum_{i=1}^{2} h_i E_i$, and $\hat{A}_h = A_h + \Delta A_h$. Then, (40) is expressed as

$$\dot{x} = \hat{A}_h x + B_w w + B\bar{u}. \tag{41}$$

Similarly, the control output (17) can be expressed as

$$z = \ddot{z}_4 = \hat{C}_h x \tag{42}$$

where $\hat{C}_h = C_h + \Delta C_h$, $C_h = \sum_{i=1}^{2} h_i C_i$, and $\Delta C_h = \sum_{i=1}^{2} h_i \Delta C_i = \sum_{i=1}^{2} h_i H_c F E_i = H_c F E_h$.

Note that the parameter uncertainties on the stiffness and damping coefficients of car and seat suspensions and sprung and unsprung masses can be dealt with in the same way, which, however, will not be further discussed here.

For the uncertain system (41) and the control output (42), (31) is also applied and can be obtained as in (43), shown at the bottom of the next page, which is further expressed as (44), also shown at the bottom of the next page. We now need the following lemma to derive the result.

Lemma 3 [32]: Given appropriately dimensioned matrices $\Sigma_1, \Sigma_2, \Sigma_3$, with $\Sigma_1^T = \Sigma_1$, then

$$\Sigma_1 + \Sigma_3 \Delta \Sigma_2 + \Sigma_2^T \Delta \Sigma_3^T < 0$$

holds for all Δ that satisfies $\Delta^T \Delta \leq I$ if and only if, for $\epsilon > 0$, we have

$$\Sigma_1 + \epsilon \Sigma_3 \Sigma_3^T + \epsilon^{-1} \Sigma_2^T \Sigma_2 < 0.$$

In fact, (44) is equivalent to

$$\Sigma_1 + \Sigma_3 F \Sigma_2 + \Sigma_2^T F \Sigma_3^T < 0 \tag{45}$$

where Σ_1 is defined in (46), shown at the bottom of the page, $\Sigma_3^T = [H_a^T \quad 0 \quad H_c^T \quad 0]$, and $\Sigma_2 = [E_h Q \quad 0 \quad 0 \quad 0]$. By using Lemma 3, we can see that the inequality (45) is satisfied if the inequality in (46) holds for $\epsilon_1 > 0$.

By the definitions $A_h = \sum_{i=1}^2 h_i A_i$ and $E_h = \sum_{i=1}^2 h_i E_i$ and the fact that $h_i \geqslant 0$ and $\sum_{i=1}^2 h_i = 1$, (46) is equivalent to (47), shown at the bottom of the page.

In addition, it is noticed that, in the aforementioned design, the driver's ride comfort is regarded as a main goal to be optimized and the vehicle suspension control is employed to achieve this goal. However, by relying on the car suspension control to optimize the head acceleration, it may possibly worsen the car suspension stroke, seat suspension stroke, and road-holding properties. Therefore, the car suspension stroke limitation, seat suspension stroke limitation, and the road-holding capability should also be considered in the controller design procedure. This case becomes a multiobjective control problem, where the following constraints should be satisfied, whereas the ride comfort performance is optimized:

$$|z_s - z_u| \leqslant z_{\max 1} \tag{48}$$
$$|z_f - z_s| \leqslant z_{\max 2} \tag{49}$$
$$k_t(z_u - z_r) < 9.8\,(m_s + m_u) \tag{50}$$

$$\begin{bmatrix} Q\hat{A}_h^T + \hat{A}_h Q + \frac{1+\varepsilon}{2}\left[C_s^T Y^T B^T + BYC_s\right] + \epsilon^{-1} BB^T & C_s^T Y^T & Q\hat{C}_h^T & B_w \\ * & -\epsilon^{-1}\left(\frac{2}{1-\varepsilon}\right)^2 I & 0 & 0 \\ * & * & -I & 0 \\ * & * & * & -\gamma^2 I \end{bmatrix} < 0 \tag{43}$$

$$\begin{bmatrix} Q(A_h+\Delta A_h)^T + (A_h+\Delta A_h)Q + \frac{1+\varepsilon}{2}\left[C_s^T Y^T B^T + BYC_s\right] + \epsilon^{-1} BB^T & C_s^T Y^T & Q(C_h+\Delta C_h)^T & B_w \\ * & -\epsilon^{-1}\left(\frac{2}{1-\varepsilon}\right)^2 I & 0 & 0 \\ * & * & -I & 0 \\ * & * & * & -\gamma^2 I \end{bmatrix} < 0 \tag{44}$$

$$\Sigma_1 = \begin{bmatrix} QA_h^T + A_h Q + \frac{1+\varepsilon}{2}\left[C_s^T Y^T B^T + BYC_s\right] + \epsilon^{-1} BB^T & C_s^T Y^T & QC_h^T & B_w \\ * & -\epsilon^{-1}\left(\frac{2}{1-\varepsilon}\right)^2 I & 0 & 0 \\ * & * & -I & 0 \\ * & * & * & -\gamma^2 I \end{bmatrix}$$
$$\times \begin{bmatrix} QA_h^T + A_h Q + \frac{1+\varepsilon}{2}\left[C_s^T Y^T B^T + BYC_s\right] + \epsilon^{-1} BB^T + \epsilon_1^{-1} H_a H_a^T & C_s^T Y^T & QC_h^T + \epsilon_1^{-1} H_a H_c^T & B_w & QE_h^T \\ * & -\epsilon^{-1}\left(\frac{2}{1-\varepsilon}\right)^2 I & 0 & 0 & 0 \\ * & * & -I & 0 & 0 \\ * & * & * & -\gamma^2 I & 0 \\ * & * & * & * & -\epsilon_1^{-1} I \end{bmatrix} < 0 \tag{46}$$

$$\begin{bmatrix} QA_i^T + A_i Q + \frac{1+\varepsilon}{2}\left[C_s^T Y^T B^T + BYC_s\right] + \epsilon^{-1} BB^T + \epsilon_1^{-1} H_a H_a^T & C_s^T Y^T & QC_i^T + \epsilon_1^{-1} H_a H_c^T & B_w & QE_i^T \\ * & -\epsilon^{-1}\left(\frac{2}{1-\varepsilon}\right)^2 I & 0 & 0 & 0 \\ * & * & -I & 0 & 0 \\ * & * & * & -\gamma^2 I & 0 \\ * & * & * & * & -\epsilon_1^{-1} I \end{bmatrix} < 0, \quad I = 1, 2 \tag{47}$$

where $z_{\max 1}$ is the maximum car suspension stroke hard limit, $z_{\max 2}$ is the maximum seat suspension stroke hard limit, and (50) indicates that the dynamic tire load should be less than the static tire load such that the wheel's contact with the ground can be kept.

To deal with these constraints, the car suspension stroke, seat suspension stroke, and tire load are defined as another control output, i.e.,

$$z_2 = \begin{bmatrix} \alpha_1(z_s - z_u)/z_{\max 1} \\ \alpha_2(z_f - z_s)/z_{\max 2} \\ \alpha_3 k_t(z_u - z_r)/9.8\,(m_{s\min} + m_u) \end{bmatrix} = C_c x \quad (51)$$

where

$$C_c = \begin{bmatrix} 0 & 0 & \frac{\alpha_1}{z_{\max 1}} & 0 & 0 & \\ 0 & 0 & 0 & 0 & \frac{\alpha_2}{z_{\max 2}} & \mathbf{0}_{3\times 11} \\ \frac{\alpha_3 k_t}{9.8(m_{s\min}+m_u)} & 0 & 0 & 0 & 0 & \end{bmatrix}.$$

In addition, α_1, α_2, and α_3 are the weighting parameters, and the performance, $\|z_2\|_\infty < \gamma\|w\|_2$, is required to be realized, where $\|z\|_\infty \triangleq \sup_{t\in[0,\infty)} \sqrt{z^T(t)z(t)}$, and $\gamma > 0$ is a performance index. Note that the weighting parameters α_1, α_2, and α_3 can properly be chosen to provide the tradeoff among different requirements such as ride comfort and road holding [33]. In general, if a small suspension stroke is required, a big weighting value for α_1 or α_2 should be chosen, and if good road-holding performance is required, a big value for α_3 should be chosen.

By using the Schur complement, the feasibility of the following inequality guarantees that $C_c^T C_c < P$:

$$\begin{bmatrix} P & C_c^T \\ C_c & I \end{bmatrix} > 0. \quad (52)$$

At the same time, based on (19) and (22), it can be derived that $x^T P x < \gamma^2 \int_0^t w^T(s)w(s)ds$ if $\Pi < 0$ is guaranteed. Then, based on (51) and (52), it can easily be established that, for all $t \geqslant 0$

$$z_2^T z_2 = x^T C_c^T C_c x < x^T P x < \gamma^2 \int_0^t w^T(s)w(s)ds$$

$$\leqslant \gamma^2 \int_0^\infty w^T(s)w(s)ds \quad (53)$$

is satisfied. Taking the supremum over $t \geqslant 0$ yields $\|z_2\|_\infty < \gamma\|w\|_2$ for all $w \in L_2[0,\infty)$. Premultiplying and postmultiplying (52) by $\mathrm{diag}(P^{-1} \quad I)$ and its transpose, respectively, and defining $Q = P^{-1}$, (52) is equivalent to

$$\begin{bmatrix} Q & QC_c^T \\ C_c Q & I \end{bmatrix} > 0. \quad (54)$$

Considering parameter uncertainties and the multiobjective control requirement, we now summarize the robust multiobjective controller design problem as follows. For given scalars, i.e., $\rho > 0$ and $\varepsilon > 0$, and matrices H_a, H_c, E_i, $i = 1, 2$, the uncertain system (41) with a controller (30) is quadratically stable, the L_2 gain that is defined by (18) is less than γ, and $\|z_2\|_\infty < \gamma\|w\|_2$ if there exist matrices $Q > 0$ and Y and scalars, i.e., $\epsilon > 0$ and $\epsilon_1 > 0$, such that the following minimization problem is feasible:

$$\min\ \gamma^2 \text{ s.t. LMIs } (32), (35), (47), \text{ and } (54). \quad (55)$$

By solving the problem of (55), the controller gain matrix can be obtained as $K = YW^{-1}$.

Note that the performance requirement that was enforced on the control output z_2 is subjected to the performance index γ and the energy of the road disturbance $\|w\|_2$. Even when γ is minimized, the constraints on the suspension stroke and the dynamic tire load may be deteriorated in practice if the road disturbance is very strong. Nevertheless, when designing a controller, an appropriate weighting on the control output z_2 can provide a good compromise among the ride comfort performance, suspension stroke limitation, and road-holding capability.

TABLE II
PARAMETER VALUES OF THE PROPOSED SUSPENSION MODEL

Mass (kg)		Damping coefficient (Ns/m)		Spring stiffness (N/m)	
m_u	20	c_t	0	k_t	180000
m_s	300	c_s	2000	k_s	10000
m_f	15	c_{ss}	830	k_{ss}	31000
m_c	1	c_c	200	k_c	18000
m_1	12.78	c_1	2064	k_1	90000
m_2	8.62	c_2	4585	k_2	162800
m_3	28.49	c_3	4750	k_3	183000
m_4	5.31	c_4	400	k_4	310000

IV. NUMERICAL SIMULATIONS

A. Validation on a Quarter-Car Model

Numerical simulations are conducted in this section to show the effectiveness of the proposed integrated seat and suspension control to improve the driver ride comfort. The parameters used in the simulations are listed in Table II, where the quarter-car suspension parameters have been optimized in terms of driver body acceleration in [22], and the seat suspension and driver body model parameters are discussed in [5].

In the simulation, the actuator force limitation for the quarter-car suspension is considered 1500 N, and for the seat suspension, the actuator force limitation is 500 N. The scalars $\varepsilon = 0.9$ and $\rho = 10^{-3}$ are chosen for designing the controllers.

To show the effectiveness and advance of the proposed control strategy, several different controllers will be designed and compared. First, we design a state feedback controller for the seat suspension model only, i.e., (3)–(8), with $k_s = 0$ and $c_s = 0$, by solving the minimization problem of (29) without considering the suspension stroke limitation and road-holding performance. The obtained controller gain matrix is given in

$$K = 10^6[-2.0237 - 0.0083 - 0.6569 - 0.0079 - 1.0691 - 0.1164$$
$$\times 1.4845 - 0.0907 3.9270 - 0.3336 8.3988 0.0792]. \quad (56)$$

This controller will use the state variables $x_5 \sim x_{16}$ of the model (9) as feedback signals in the simulation and is denoted as controller 1 for description simplicity.

Then, we design another state feedback controller for the quarter-car suspension model only, i.e., (1) and (2), with $k_{ss} = 0$, $c_{ss} = 0$, and $u_f = 0$, by solving the minimization problem of (29) without considering the suspension stroke limitation and road-holding performance. The obtained controller gain matrix is given as

$$K = 10^3[0.4456 \; -1.8543 \; 9.5208 \; 1.1960]. \tag{57}$$

This controller will use the state variables $x_1 \sim x_4$ of the model (9) as feedback signals in the simulation and is denoted as controller 2 for description simplicity.

Then, we design a state feedback controller for the integrated seat and suspension model, i.e., (1)–(8), by solving the minimization problem of (29) without considering the suspension stroke limitation and road-holding performance. The obtained controller gain matrix is given as

$$\begin{aligned} K = 10^6[&\text{-}0.0061 \; -0.0000 \; -0.0052 \; -0.0006 \; 0.0198 \\ &-0.0035 \; 0.2834 \; -0.0021 \; 0.2195 \; -0.0280 \; 0.9059 \\ &-0.0119 \; 1.1534 \; 0.0101 \; -26.103 \; 0.0284; 0.0553 \\ &-0.0001 \; 0.0041 \; -0.0096 \; 0.1501 \; -0.0015 \; 0.1983 \\ &-0.0000 \; 0.1636 \; 0.0002 \; 0.0564 \; 0.0021 \\ &-0.0954 \; 0.0162 \; -3.4882 \; -0.0085]. \end{aligned} \tag{58}$$

This controller will use the state variables $x_1 \sim x_{16}$ of the model (9) as feedback signals in the simulation and is denoted as controller 3 for description simplicity. This controller will provide two control inputs to the seat suspension and car suspension, respectively.

To validate the suspension performance in the time domain, two typical road disturbances, i.e., bump road disturbance and random road disturbance, will be considered in the simulation and applied to the vehicle wheel.

1) Comparison on Bump Response: The ground displacement for an isolated bump in an otherwise smooth road surface is given by

$$z_r(t) = \begin{cases} \frac{a}{2}\left(1 - \cos\left(\frac{2\pi v_0}{l}t\right)\right), & 0 \leqslant t \leqslant \frac{l}{v_0} \\ 0, & t > \frac{l}{v_0} \end{cases} \tag{59}$$

where a and l are the height and the length of the bump, respectively, and v_0 is the vehicle forward speed. We choose $a = 0.1$ m, $l = 2$ m, and $v_0 = 30$ km/h in the simulation.

The bump responses of the driver head acceleration for the integrated seat and suspension system with different controllers are compared in Fig. 2, where Passive means that no controller has been used, Active Seat means that controller 1 is used for seat suspension only, Active Suspension means that controller 2 is used for car suspension only, and Integrated means that controller 3 is used for both seat suspension and car suspension. In Fig. 2, it is shown that the Integrated control achieves the best performance among all the compared control strategies on ride comfort in terms of the peak value of driver head acceleration. Further comparison on the control forces is shown in Fig. 3, where the integrated control provides two control forces, which are denoted as Active Seat and Active Suspension to the seat suspension and the car suspension, respectively.

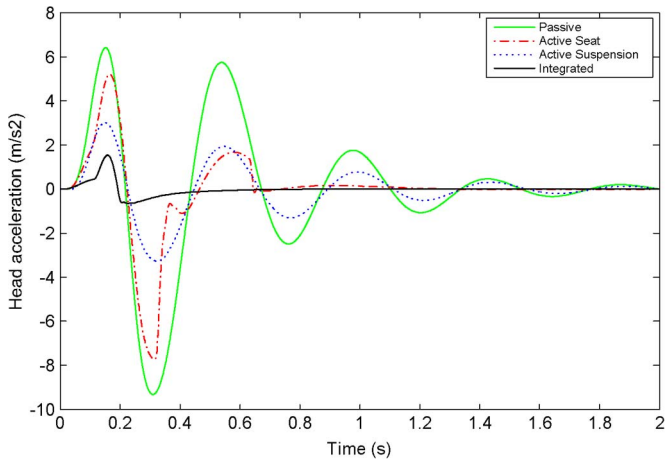

Fig. 2. Bump responses on driver head acceleration for different control systems.

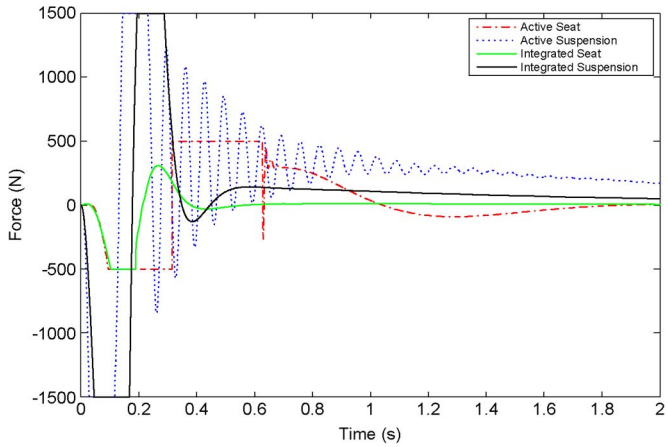

Fig. 3. Control forces under bump road disturbance.

As stated previously, the state feedback controller is not practically realizable, particularly when the human body model is included. We now design a static output feedback controller for the integrated seat and suspension model (1)–(8) by solving the minimization problem of (36) without considering the suspension stroke limitation and road-holding performance. By assuming that all the state variables for car suspension and seat suspension are available for measurement by using displacement and velocity sensors or using accelerometers with integration functions and all the state variables for the driver body model are not measurement available, the controller gain matrix is obtained as in (60), shown at the bottom of the page. This controller uses only the measurement available state

$$K = 10^5 \begin{bmatrix} \text{-}0.4665 & 0.0000 & -0.4759 & -0.0080 & -0.1965 & -0.1023 & 8.6420 & -0.1991 \\ 8.2020 & 0.0171 & 1.4630 & -0.1564 & 9.4831 & 0.0284 & 6.1010 & 0.1435 \end{bmatrix} \tag{60}$$

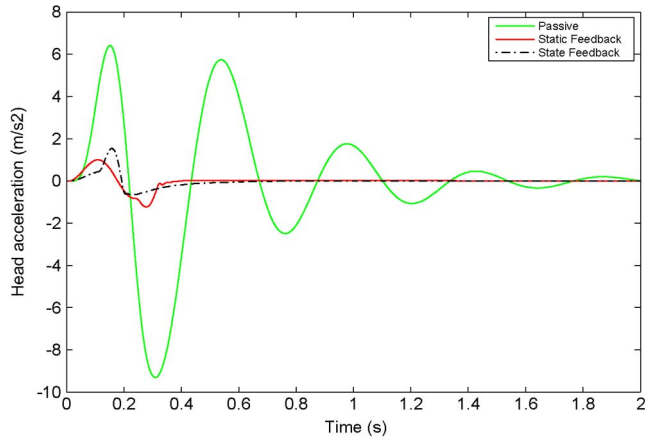

Fig. 4. Bump responses on driver head acceleration for state feedback control and static output feedback control.

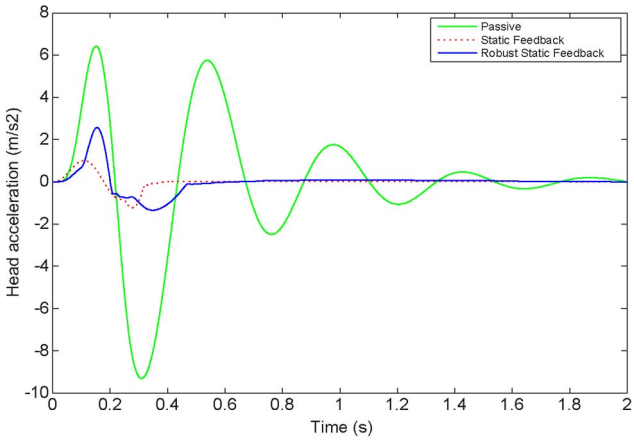

Fig. 6. Bump responses on driver head acceleration for static feedback control and robust static output feedback control.

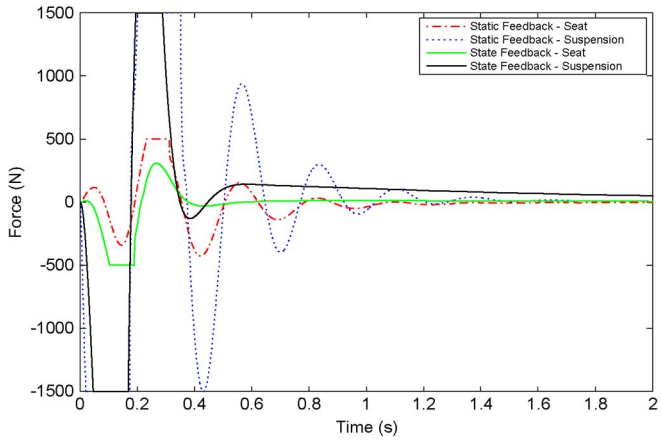

Fig. 5. Control forces under bump road disturbance for state feedback control and static output feedback control.

variables $x_1 \sim x_8$ of the model (9) as feedback signals in the simulation and is denoted as controller 4 for description simplicity.

To clearly show the performance of the designed static output feedback controller, the bump responses on driver head acceleration for the integrated seat and suspension system with no controller, state feedback controller, and static output feedback controller are compared in Fig. 4, where State Feedback means that controller 3 is used, and Static Feedback means that controller 4 is used. In Fig. 4, it is shown that the static output feedback controller achieves similar performance to the state feedback controller in terms of the peak value on driver head acceleration despite its simple structure. The comparison on the control forces is shown in Fig. 5. In Fig. 5, it is shown that both the state feedback controller and the static output feedback controller provide two control forces to the system and that their forces to seat suspension and car suspension are quite similar.

It is noticed that controller 4 achieves good ride comfort performance with limited information. However, for vehicle suspension, aside from the ride comfort that needs to be focused on, the car and seat suspension stroke limitation and road-holding performance also need to be considered. In addition, parameter uncertainties, which may often happen to the system in practice, should also be dealt with. Furthermore, the measurement of tire deflection x_1 and velocity x_2 may not be easily available in practice. Therefore, a robust controller that compromises the performance among ride comfort, car and seat suspension stroke limitation, and road-holding capability and considers parameter uncertainties and measurement availability is finally designed by solving the problem of (55). The obtained controller gain matrix is given as (61), shown at the bottom of the page, which uses the measurement available state variables $x_3 \sim x_8$ of the model (9) as feedback signals and is denoted as controller 5 for description simplicity.

To show the difference between controllers 4 and 5 on different performance aspects, the driver head acceleration, car suspension stroke, seat suspension stroke, and dynamic tire load under bump road input are shown in Figs. 6–9, respectively. It is shown that controller 4, which is indicated as Static Feedback in the figures, achieves better ride comfort in terms of the peak value on driver head acceleration in Fig. 6 compared with controller 5, which is indicated as Robust Static Feedback. However, it generates bigger suspension stroke and dynamic tire load, as shown in Figs. 7 and 9, compared with controller 5. This condition may result in suspension end-stop collision and cause the wheels to lift off the ground. The dynamic tire load of controller 5 is quite similar to the passive suspension in terms of the maximum peak value. Although controller 5 requires bigger seat suspension stroke than controller 4 and passive suspension, in Fig. 8, it is observed that the stroke is still within ± 20 mm, which is acceptable for seat suspension [34]. Therefore, controller 5 achieves a good tradeoff among

$$K = 10^5 \begin{bmatrix} 0.0661 & 0.0065 & -0.2115 & 0.0336 & -2.7173 & -0.0167 \\ -0.1255 & 0.0378 & -0.3292 & -0.0205 & 1.3831 & 0.0042 \end{bmatrix} \tag{61}$$

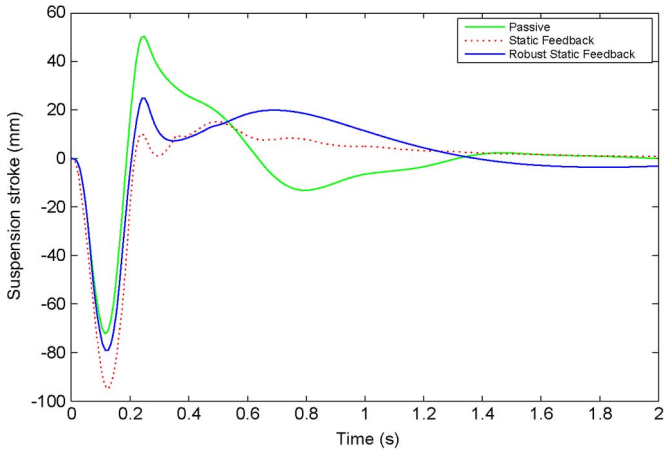

Fig. 7. Bump responses on car suspension stroke for static feedback control and robust static output feedback control.

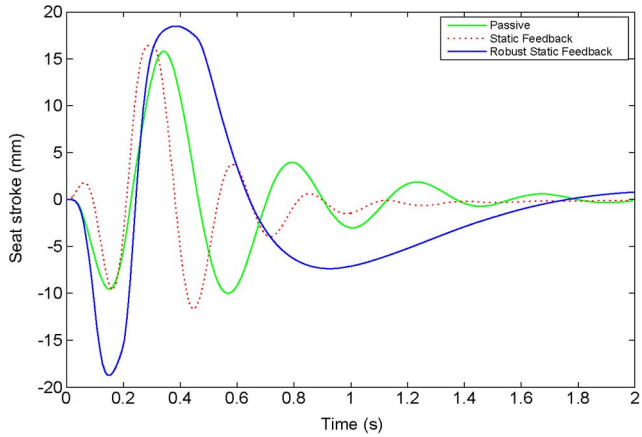

Fig. 8. Bump responses on seat suspension stroke for static feedback control and robust static output feedback control.

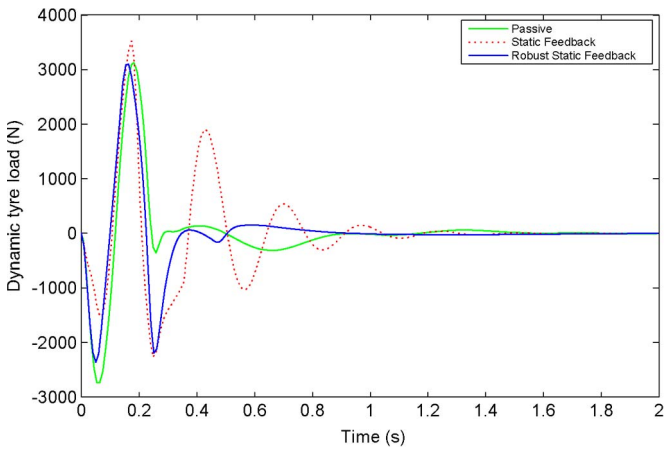

Fig. 9. Bump responses on dynamic tire load for static feedback control and robust static output feedback control.

different performance requirements. This controller will further be tested on a full-car model in the next section.

On the other hand, from an implementation point of view, note that, for a real vehicle, the aforementioned controller can be integrated into a suspension control module, which is designed as an embedded electronic control unit that controls one or more of the electrical systems in a car. This module will receive signals from sensors that were installed at wheels and seat frame and calculate the required control forces in terms of the designed controller gain matrix. The control forces will then be generated by the actuators and applied to the vehicle and seat. Note that the controller gain matrix is a constant matrix that does not need to be recalculated in a real-time implementation and can easily be stored in a microprocessor memory [random access memory or read-only memory]. The calculation of the control forces is straightforward, without high computational power. This condition enables the implementation of the controller on a microcontroller board.

Comparison on Random Response: When the road disturbance is considered as vibration, it is typically specified as a random process with a ground displacement power spectral density of

$$S_g(\Omega) = \begin{cases} S_g(\Omega_0)\left(\frac{\Omega}{\Omega_0}\right)^{-n_1}, & \text{if } \Omega \le \Omega_0 \\ S_g(\Omega_0)\left(\frac{\Omega}{\Omega_0}\right)^{-n_2}, & \text{if } \Omega \ge \Omega_0 \end{cases} \tag{62}$$

where $\Omega_0 = (1/2\pi)$ is a reference frequency, Ω is a frequency, and n_1 and n_2 are road roughness constants. The value $S_g(\Omega_0)$ provides a measure for the roughness of the road. In particular, samples of the random road profile can be generated using the spectral representation method [35]. If the vehicle is assumed to travel with a constant horizontal speed v_0 over a given road, the road irregularities can be simulated by the following series:

$$z_r(t) = \sum_{n=1}^{N_f} s_n \sin(n\omega_0 t + \varphi_n) \tag{63}$$

where $s_n = \sqrt{2S_g(n\triangle\Omega)\triangle\Omega}$, $\triangle\Omega = (2\pi/l)$, l is the length of the road segment, $\omega_0 = (2\pi/l)v_0$, and φ_n is treated as random variables that follow uniform distribution in the interval $[0, 2\pi)$. N_f limits the considered frequency range.

To validate the effectiveness of controller 5 under different road conditions and different vehicle speeds, we use $n_1 = 2$, $n_2 = 1.5$, $l = 200$, and $N_f = 200$ in (62) and (63), select the road roughness as $S_g(\Omega_0) = 64 \times 10^{-6}$ m^3 (C grade, average), $S_g(\Omega_0) = 256 \times 10^{-6}$ m^3 (D grade, poor), and $S_g(\Omega_0) = 1024 \times 10^{-6}$ m^3 (E grade, very poor), respectively, according to ISO 2631 standards, and choose speed from 60 km/h to 100 km/h, with an interval of 10 km/h. Taking into account the random nature of the road input, the root-mean-square (RMS) values of the driver head acceleration, car suspension stroke, seat suspension stroke, and dynamic tire load are used as performance indices to compare the performance of integrated active suspension and passive suspension. The simulation will randomly be run 100 times to calculate the expectation of RMS values, and the results under three different road profiles and five different speeds are compared in Figs. 10–12. In Figs. 10–12, it can be observed that integrated static output feedback controller 5 always outperforms the passive suspension in terms of head acceleration with practically accepted car suspension stroke, seat suspension stroke, and dynamic tire load despite the change of road conditions and speed. To more

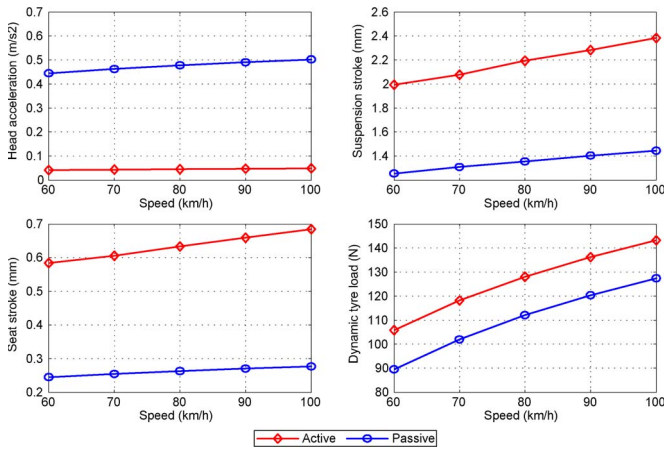

Fig. 10. RMS of random responses under C-grade road disturbance with different vehicle speed levels.

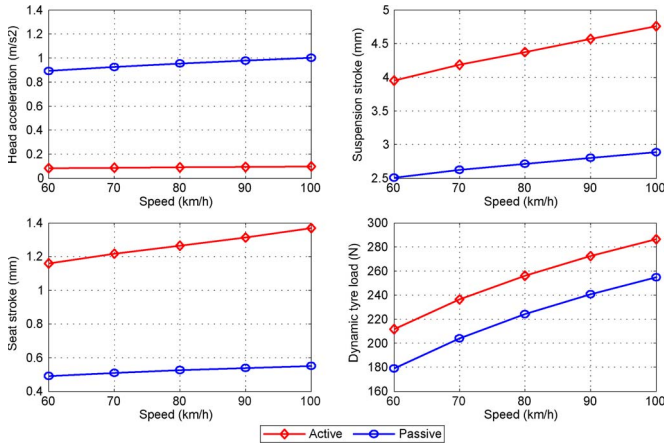

Fig. 11. RMS of random responses under D-grade road disturbance with different vehicle speed levels.

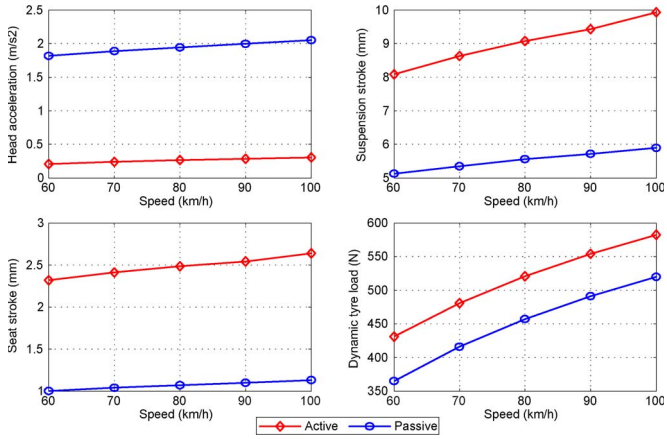

Fig. 12. RMS of random responses under E-grade road disturbance with different vehicle speed levels.

clearly show the results, one sample of random responses under D-grade road disturbance with a vehicle speed of 100 km/h is shown in Fig. 13. In Fig. 13, it is shown that the head acceleration is really improved by integrated active suspension compared with passive suspension.

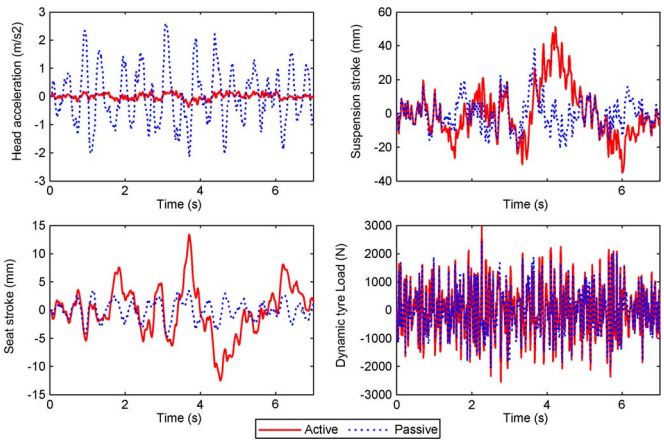

Fig. 13. Random responses under D-grade road disturbance with a vehicle speed of 100 km/h.

B. *Validation on a Full-Car Model*

Although the proposed controller is designed for a quarter-car model, it is now applied to a full-car model to further validate its effectiveness and robustness to actuator dynamics, measurement noises, and parameter uncertainties. A full-car suspension model together with a seat suspension model and a driver body is shown in Fig. 14, where $m_s = 1200$ kg, $I_\theta = 2100$ kg m^2, $I_\phi = 460$ kg m^2, $l_f = 1.011$ m, $l_r = 1.803$ m, $t_f = 0.761$ m, $t_r = 0.761$ m, $s_x = 0.3$ m, and $s_y = 0.25$ m [7]. The driver seat and body models are the same as described in Fig. 1. Furthermore, four electrohydraulic actuators are assumed to be installed between unsprung and sprung masses, and one electrohydraulic actuator is placed between the cabin floor and the seat frame. The electrohydraulic actuator is modeled as [33]

$$\frac{V_t}{4\beta_e}\dot{P}_L = Q_L - C_{tp}P_L - A_r(\dot{x}_s - \dot{x}_u) \tag{64}$$

where P_L is the pressure drop across the piston, A_r is the piston area of the hydraulic actuator, β_e is the effective bulk modulus, V_t is the total actuator volume, C_{tp} is the coefficient of the total leakage due to pressure, and Q_L is the load flow. The parameter values are given as $A_r = 3.35 \times 10^{-4}$ m^2, $(V_t/4\beta_e) = 4.515 \times 10^{13}$ N/m^5, and $C_{tp} = (4\beta_e/V_t)$.

To validate the system performance, the bump road disturbances as shown in Fig. 15 will be applied to the vehicle wheels. Fig. 15 shows that the road disturbances, which are applied to the front and rear wheels, have the same peak amplitude, with a time delay of $(l_f + l_r)/v_0$. However, to excite the roll motion of the vehicle, the road disturbances to the left and right wheels are applied with different amplitude [7].

In the simulation, the designed controller 5 will be applied to calculate the desired control force in terms of the measured signals for each actuator, and then, the desired forces will be tracked and applied to the vehicle and seat suspension through electrohydraulic actuators. For simplicity, a proportional–integral–derivative controller will be applied to each actuator as an inner control loop so that each actuator can track its desired force. More advanced strategies for controlling electrohydraulic actuators can be found, for example, in [36] and [37], which, however, will not be discussed in this paper.

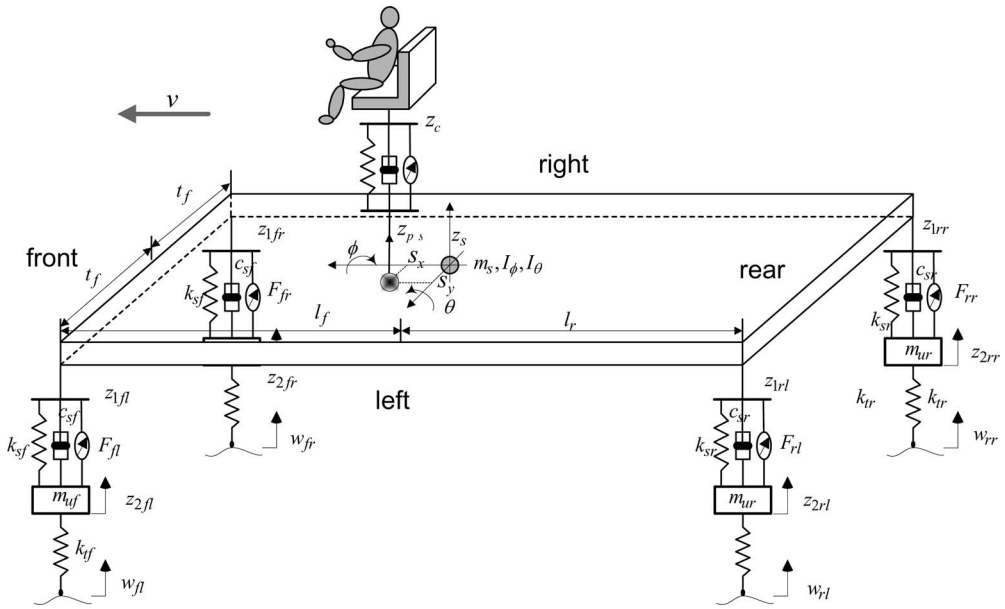

Fig. 14. Full-car suspension model with a driver seat.

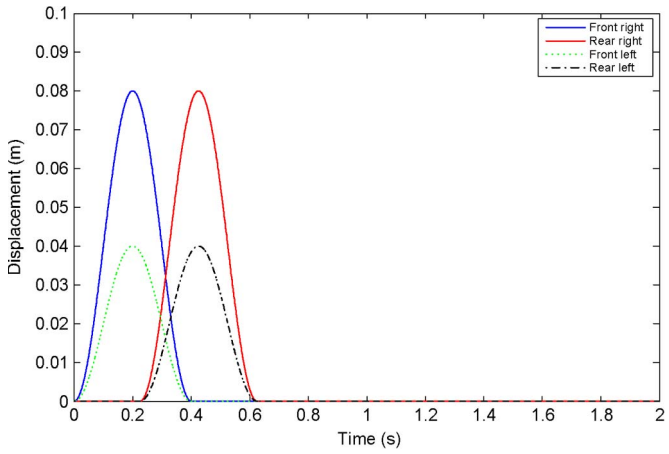

Fig. 15. Road disturbance.

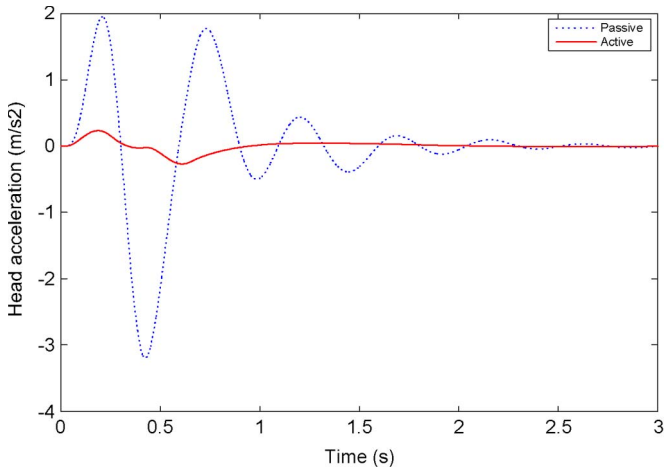

Fig. 16. Bump responses on driver head acceleration for a full-car suspension without parameter uncertainties and measurement noises.

First, we assume that the system does not have parameter uncertainties and measurement noises. When controller 5 is applied, the driver head acceleration under the bump road

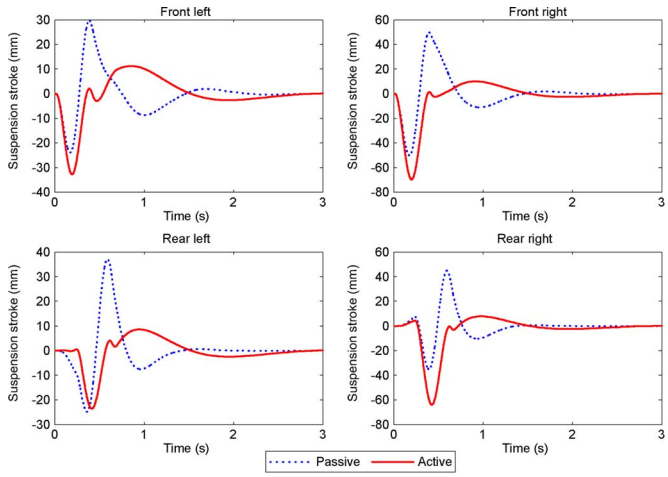

Fig. 17. Car suspension strokes under bump road disturbances.

disturbance is shown in Fig. 16. In Fig. 16, it is shown that the proposed control strategy largely reduces the driver head acceleration compared to the passive system and therefore achieves good ride comfort performance. The car suspension stroke, seat suspension stroke, and dynamic tire load are compared with the passive system in Figs. 17–19, respectively. It is shown that all the strokes are within their limitations under this bump road input, and their dynamic tire loads show that the road-holding performance is kept. The actuator output forces are shown in Fig. 20, where the seat suspension actuator provides less force compared with the wheel suspension actuators.

Under the random road disturbance, the RMS values under three different road profiles and five different speeds are also calculated. For brevity, only the results under E-grade road disturbance with different speed levels are shown in Fig. 21. A similar conclusion can be obtained in Fig. 21, i.e., integrated static output feedback controller 5 outperforms the passive suspension in terms of head acceleration with practically accepted car suspension stroke, seat suspension stroke, and dynamic tire load, despite the change of speed. One sample of random

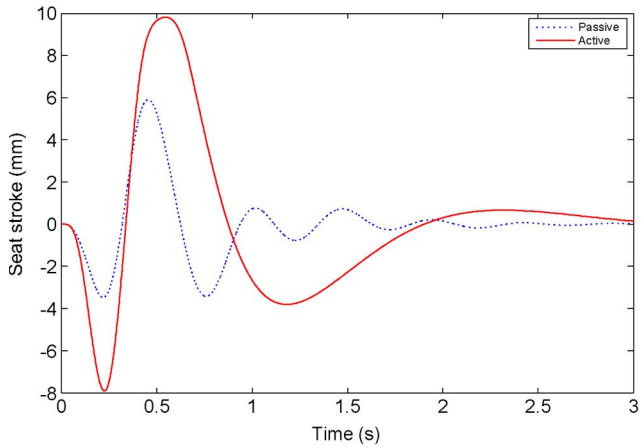

Fig. 18. Seat suspension strokes under bump road disturbances.

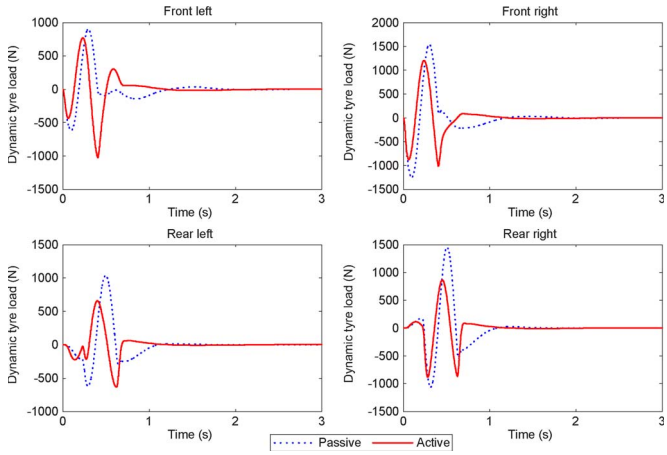

Fig. 19. Dynamic tire loads under bump road disturbances.

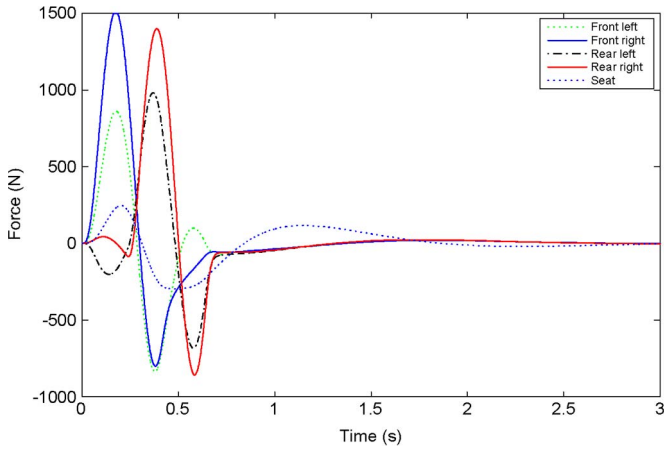

Fig. 20. Actuator output forces under bump road disturbances.

responses under D-grade road disturbance with a vehicle speed 100 km/h is shown in Fig. 22, which also confirms the effectiveness of the designed controller.

Last, parameter uncertainties to the driver body model and measurement noises on wheel vertical accelerations, which will be integrated to get wheel velocities and displacements, are added to the full-car model. The variations to the driver's mass, stiffness, and damping coefficients are randomly generated within 10% of their nominal values. Many cases have been tested; however, to save space, only one case with the driver

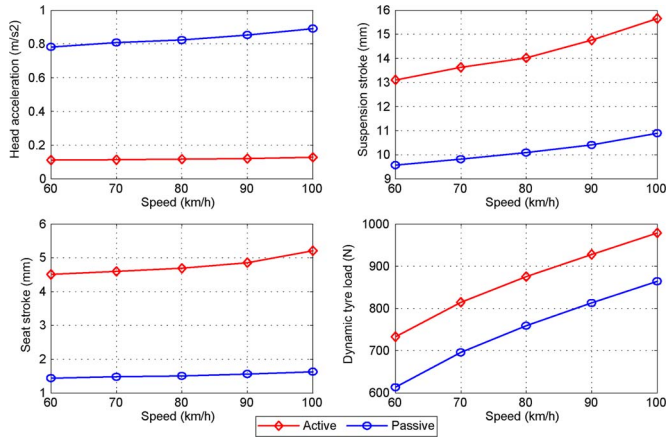

Fig. 21. RMS of random responses under E-grade road disturbance with different vehicle speed levels.

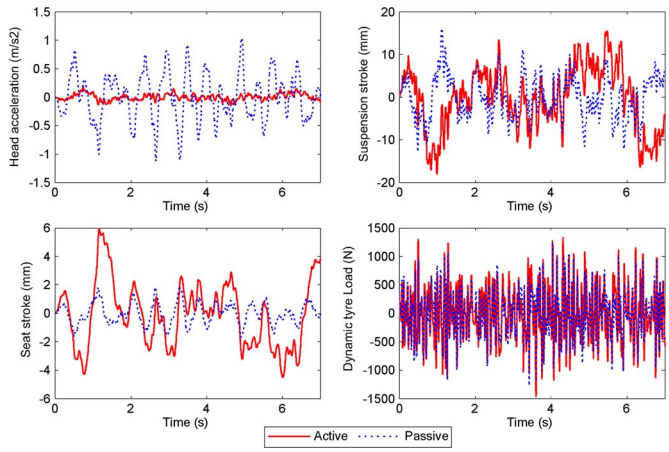

Fig. 22. Random responses under D-grade road disturbance with a vehicle speed of 100 km/h.

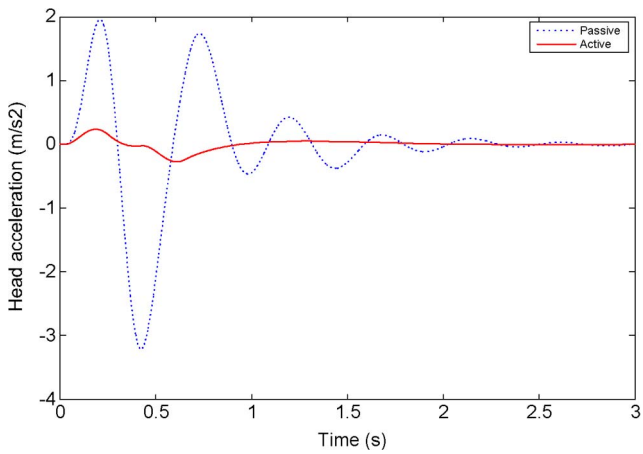

Fig. 23. Bump responses on driver head acceleration for a full-car suspension with parameter uncertainties and measurement noises.

head acceleration under the bump road disturbance is shown in Fig. 23, and the noised wheel accelerations are shown in Fig. 24. In Fig. 23, it is shown that the proposed control strategy reduces the driver head acceleration compared with the passive system, even when there exist parameter uncertainties and measurement noises. The robustness of the designed controller is validated to be effective.

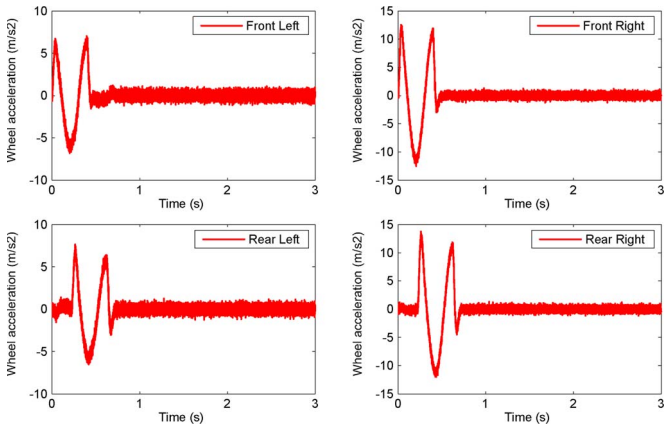

Fig. 24. Wheel vertical accelerations with measurement noises.

V. Conclusion

In this paper, an integrated seat and suspension has been developed and used for an integrated controller design. Because some state variables are not measurement available in practice, a static output feedback controller design method has been presented. Considering the limited capability of actuators, the actuator saturation constraint is included in the controller design process. Numerical simulations are used to validate the performance of the designed controllers. The results show that the integrated seat and suspension control can provide the best ride comfort performance compared with the passive seat and suspension, active seat suspension control, and active car suspension control. The static output feedback control achieves compatible performance to the state feedback control with a realizable structure. Further study on the robust control of the integrated model, considering more complex car models, actuator dynamics, time-varying parameters and parameter uncertainties, and measurement noise, will be conducted.

Acknowledgment

The authors would like to thank the anonymous reviewers for their invaluable suggestions and comments on the improvement of this paper.

References

[1] S.-B. Choi, M.-H. Nam, and B.-K. Lee, "Vibration control of a MR seat damper for commercial vehicle," *J. Intell. Mater. Syst. Struct.*, vol. 11, no. 12, pp. 936–944, Dec. 2000.

[2] I. J. Tiemessen, C. T. J. Hulshof, and M. H. W. Frings-Dresen, "An overview of strategies to reduce whole-body vibration exposure on drivers: A systematic review," *Int. J. Ind. Ergonom.*, vol. 37, no. 3, pp. 245–256, Mar. 2007.

[3] C.-M. Lee, A. H. Bogatchenkov, V. N. Goverdovskiy, Y. V. Shynkarenko, and A. I. Temnikov, "Position control of seat suspension with minimum stiffness," *J. Sound Vib.*, vol. 292, no. 1/2, pp. 435–442, Apr. 2006.

[4] Y. Wan and J. M. Schimmels, "Improved vibration isolating seat suspension designs based on position-dependent nonlinear stiffness and damping characteristics," *J. Dyn. Syst., Meas. Control*, vol. 125, no. 3, pp. 330–338, 2003.

[5] S.-B. Choi and Y.-M. Han, "Vibration control of electrorheological seat suspension with human-body model using sliding mode control," *J. Sound Vib.*, vol. 303, no. 1/2, pp. 391–404, Jun. 2007.

[6] J.-D. Wu and R.-J. Chen, "Application of an active controller for reducing small amplitude vertical vibration in a vehicle seat," *J. Sound Vib.*, vol. 274, no. 3–5, pp. 939–951, Jul. 2004.

[7] M. Bouazara, M. J. Richard, and S. Rakheja, "Safety and comfort analysis of a 3-D vehicle model with optimal nonlinear active seat suspension," *J. Terramechanics*, vol. 43, no. 2, pp. 97–118, 2006.

[8] I. Maciejewski, L. Meyer, and T. Krzyzynski, "The vibration damping effectiveness of an active seat suspension system and its robustness to varying mass loading," *J. Sound Vib.*, vol. 329, no. 19, pp. 3898–3914, Sep. 2010.

[9] Y. Zhao, L. Zhao, and H. Gao, "Vibration control of seat suspension using H_∞ reliable control," *J. Vib. Control*, vol. 16, no. 12, pp. 1859–1879, Oct. 2010.

[10] Y. Zhao, W. Sun, and H. Gao, "Robust control synthesis for seat suspension systems with actuator saturation and time-varying input delay," *J. Sound Vib.*, vol. 329, no. 21, pp. 4335–4353, Oct. 2010.

[11] W. Sun, J. Li, Y. Zhao, and H. Gao, "Vibration control for active seat suspension systems via dynamic output feedback with limited-frequency characteristic," *Mechatronics*, vol. 21, no. 1, pp. 250–260, Feb. 2011.

[12] D. Hrovat, "Survey of advanced suspension developments and related optimal control applications," *Automatica*, vol. 33, no. 10, pp. 1781–1817, Oct. 1997.

[13] R. A. Williams, "Automotive active suspensions," *Proc. Inst. Mech. Eng.: Part D—J. Autom. Eng.*, vol. 211, no. 6, pp. 415–444, 1997.

[14] S.-K. Chung and H.-B. Shin, "High-voltage power supply for semiactive suspension system with ER-fluid damper," *IEEE Trans. Veh. Technol.*, vol. 53, no. 1, pp. 206–214, Jan. 2004.

[15] E. Guglielmino, T. Sireteanu, C. W. Stammers, G. Ghita, and M. Giuclea, *Semiactive Suspension Control—Improved Vehicle Ride and Road Friendliness*. London, U.K.: Springer-Verlag, 2008.

[16] I. Martins, J. Esteves, G. D. Marques, and F. Pina da Silva, "Permanent-magnet linear actuators applicability in automobile active suspensions," *IEEE Trans. Veh. Technol.*, vol. 55, no. 1, pp. 86–94, Jan. 2006.

[17] B. L. J. Gysen, J. J. H. Paulides, J. L. G. Janssen, and E. A. Lomonova, "Active electromagnetic suspension system for improved vehicle dynamics," *IEEE Trans. Veh. Technol.*, vol. 59, no. 3, pp. 1156–1163, Mar. 2010.

[18] B. L. J. Gysen, T. P. J. van der Sande, J. J. H. Paulides, and E. A. Lomonova, "Efficiency of a regenerative direct-drive electromagnetic active suspension," *IEEE Trans. Veh. Technol.*, vol. 60, no. 4, pp. 1384–1393, May 2011.

[19] J. Wang, W. Wang, and K. Atallah, "A linear permanent-magnet motor for active vehicle suspension," *IEEE Trans. Veh. Technol.*, vol. 60, no. 1, pp. 55–63, Jan. 2011.

[20] Z. Zhang, N. C. Cheung, K. W. E. Cheng, X. Xue, and J. Lin, "Direct instantaneous force control with improved efficiency for four-quadrant operation of linear switched reluctance actuator in active suspension system," *IEEE Trans. Veh. Technol.*, vol. 61, no. 4, pp. 1567–1576, May 2012.

[21] O. Gundogdu, "Optimal seat and suspension design for a quarter car with driver model using genetic algorithms," *Int. J. Ind. Ergonom.*, vol. 37, no. 4, pp. 327–332, Apr. 2007.

[22] A. Kuznetsov, M. Mammadov, I. Sultan, and E. Hajilarov, "Optimization of a quarter-car suspension model coupled with the driver biomechanical effects," *J. Sound Vib.*, vol. 330, no. 12, pp. 2937–2946, Jun. 2011.

[23] H. Du, N. Zhang, and J. Lam, "Parameter dependent input-delayed control of uncertain vehicle suspensions," *J. Sound Vib.*, vol. 317, no. 3, pp. 537–556, Nov. 2008.

[24] J. H. Kim and F. Jabbari, "Actuator saturation and control design for buildings under seismic excitation," *J. Eng. Mech.*, vol. 128, no. 4, pp. 403–412, Apr. 2002.

[25] K. Zhou and P. P. Khargonekar, "An algebraic Riccati equation approach to H_∞ optimization," *Syst. Control Lett.*, vol. 11, no. 2, pp. 85–91, Aug. 1988.

[26] S. Boyd, L. El Ghaoui, E. Feron, and V. Balakrishnan, *Linear Matrix Inequalities in System and Control Theory*. Philadelphia, PA: SIAM, Jun. 1994.

[27] Y.-Y. Cao and Z. Lin, "Robust stability analysis and fuzzy-scheduling control for nonlinear systems subject to actuator saturation," *IEEE Trans. Fuzzy Syst.*, vol. 11, no. 1, pp. 57–67, Feb. 2003.

[28] V. L. Syrmos, C. T. Abdallah, P. Dorato, and K. Grigoriadis, "Static output feedback—A survey," *Automatica*, vol. 33, no. 2, pp. 125–137, Feb. 1997.

[29] H. Du and N. Zhang, "Designing H_∞/GH_2 static-output feedback controller for vehicle suspensions using linear matrix inequalities and genetic algorithms," *Veh. Syst. Dyn.*, vol. 46, no. 5, pp. 385–412, 2008.

[30] H. Du and N. Zhang, "Static output feedback control for electrohydraulic active suspensions via TS fuzzy model approach," *J. Dyn. Syst., Meas., Control*, vol. 131, no. 5, pp. 051004-1–051004-11, 2009.

[31] D. W. C. Ho and Y. Niu, "Robust fuzzy design for nonlinear uncertain stochastic systems via sliding-mode control," *IEEE Trans. Fuzzy Syst.*, vol. 15, no. 3, pp. 350–358, Jun. 2007.

[32] H. Gao and T. Chen, "Network-based H_∞ output tracking control," *IEEE Trans. Autom. Control*, vol. 53, no. 3, pp. 655–667, Apr. 2008.
[33] H. Chen and K. Guo, "Constrained H_∞ control of active suspensions: An LMI approach," *IEEE Trans. Control Syst. Technol.*, vol. 13, no. 3, pp. 412–421, May 2005.
[34] I. Maciejewskia, L. Meyerb, and T. Krzyzynski, "Modeling and multicriteria optimization of passive seat suspension vibroisolating properties," *J. Sound Vib.*, vol. 324, no. 3–5, pp. 520–538, Jul. 2009.
[35] G. Verros, S. Natsiavas, and C. Papadimitriou, "Design optimization of quarter-car models with passive and semiactive suspensions under random road excitation," *J. Vib. Control*, vol. 11, no. 5, pp. 581–606, May 2005.
[36] A. Alleyne and R. Liu, "Systematic control of a class of nonlinear systems with application to electrohydraulic cylinder pressure control," *IEEE Trans. Control Syst. Technol.*, vol. 8, no. 4, pp. 623–634, Jul. 2000.
[37] A. G. Thompson and B. R. Davis, "Force control in electrohydraulic active suspensions revisited," *Veh. Syst. Dyn.*, vol. 35, no. 3, pp. 217–222, 2001.

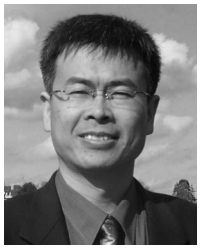

Haiping Du received the Ph.D. degree in mechanical design and theory from Shanghai Jiao Tong University, Shanghai, China, in 2002.

From 2005 to 2009, he was a Research Fellow with the Faculty of Engineering, University of Technology, Sydney, NSW, Australia. From 2004 to 2005, he was a Postdoctoral Research Associate with the Imperial College London, U.K. From 2002 to 2003, he was with the University of Hong Kong, Pokfulam, Hong Kong. He is currently a Senior Lecturer with the School of Electrical, Computer and Telecommunications Engineering, University of Wollongong, Wollongong, NSW, Australia. His research interests include vehicle dynamics and control, robust control theory and engineering applications, soft computing, model and controller reduction, and smart materials and structures.

Weihua Li received the B.Eng. and M.Eng. degrees from the University of Science and Technology of China, Hefei, China, in 1992 and 1995, respectively, and the Ph.D. degree from Nanyang Technological University (NTU), Singapore, in 2001.

For two years, he was with NTU for postdoctoral training. Then, he joined the University of Wollongong (UOW), Wollongong, NSW, Australia, as a full-time academic. He is currently the Director of Engineering Manufacturing Research Strength and the Discipline Advisor for Mechatronic Engineering with the School of Mechanical, Materials and Mechatronic Engineering, UOW. He is currently an Editorial Board Member for more than eight international journals. He has been a coauthor of more than 160 articles and has delivered many plenary or invited talks at various international conferences. His research interests include smart materials and structures, microfluidics, intelligent mechatronics, and dynamics and vibration control.

Nong Zhang received the B.E. degree from the Northeastern University, Shenyang, China, in 1982, the M.E. degree from Shanghai Jiao Tong University, Shanghai, China, in 1984, and the Ph.D. degree from the University of Tokyo, Tokyo, Japan, in 1989.

He has been with several prestigious universities in China, Japan, the United States, and Australia, respectively. In 1995, he joined the Faculty of Engineering and Information Technology, University of Technology, Sydney, NSW, Australia, where he has been a Professor of mechanical engineering with the School of Electrical, Mechanical and Mechatronic Systems since 2009. His research interests include the dynamics and control of automotive systems, particularly powertrains with various types of transmissions, hybrid propulsion systems for hybrid electric vehicles, vehicle dynamics, and passive and active suspensions, as well as mechanical vibration, particularly experimental modal analysis, rotor dynamics, and cold rolling mill chatter.